Phenomenological theory of the dielectric response of lead magnesium niobate and lead scandium tantalate

by

H. Qian and L.A. Bursill

School of Physics, The University of Melbourne, Parkville, Vic., 3052
Australia

Received

Abstract

The influence of the random field effects originating from charged chemical defects and nano-domain textures on the formation and dynamics of polar clusters is analyzed. The spatial distribution of the local fields is not totally random but contains some correlations in direction and strength. Polar clusters are classified to be dynamic or frozen according to their dynamic characteristics in the random fields. The relaxation formula of a dipolar moment in an anisotropic double-well potential is deduced. Two percolation models are introduced, one to account for frustration effects associated with multiple orientations of polar clusters, which results in a broad diffuse dielectric response and the second to account for the case whereby there may be a phase transition to a ferroelectric state. The dielectric permittivity and dissipation factor of the typical relaxors lead magnesium niobate and lead scandium tantalate are predicted as a function of both temperature and frequency, which results are in good agreement with the experimental measurements.

1. Introduction

Relaxor ferroelectrics exhibit the following typical characteristics[1,2]: a significant frequency-dependence of the peak permittivity; a ferroelectric response under high electric fields at lower temperature; but no macroscopic spontaneous polarization and anisotropy in the zero-field-cooled state. We

take $PbMg_{1/3}Nb_{2/3}$ (PMN) as an example in our discussion, because it is the archetype relaxor. It has been shown that PMN has a compositionally disordered structure characterised by nanometer scale 1:1 ordering of Mg^{2+} and Nb^{5+} on the B-sites of the perovskite structure ABO_3[3,4]. Presumably this charge distribution generates local electric fields with more or less random direction and dispersive strength. Cross[1,2] suggested that this nano-meter scale chemical structure will limit the size of polar moments so that their orientations may be thermally agitated and hence exhibit super-paraelectric characteristics. Viehland et. al. [5–9] proposed that a polar glass state will develop among the clusters and used the Vogel–Fulcher relationship successfully in explaining the experimental results on the dielectric relaxation. Westphal and Kleemann[10,11] proposed that it is the random-fields due to the disordered distribution of the B-site cations that stabilize the nano-domain state rather than the development of a polar glassy state.

Recently the present authors[12–14] have studied the chemical nano-domain structures and textures of $Pb(Sc_{1/2}Ta_{1/2})O_3$ (PST) and PMN with high resolution TEM and computer simulations. Atomic models for the distribution of B-site cations were proposed, based upon the results of extended Next Nearest Neighbour Ising model simulations. These models were used to analyse high-resolution transmission electron microscopy (HRTEM) observations of the chemical domain strucxtures of PST and PMN[12–13], thus providing realistic atomic models for these complex disordered systems for the first time since their discovery by Smolenskii and Isupov[15]. Based on these models we may also obtain some detailed information on the statistical distribution of the domain size for different methods of specimen preparation.

In this paper, we develop a phenomenological theory of the dielectric response of PMN and PST, based on a new understanding of the role of charged chemical defects and the existence of more or less random dipolar fields associated with these inhomogeneities. In Sec. 2 the influence of the random fields, originated from charged chemical nano-domains, on the formation and dynamics of polar clusters is further analyzed. Two kinds of polar clusters are assumed. The scaling behaviours of these clusters and their relation to the the frozen chemical nano-domain texture and structures are discussed. Two kinds of competing percolations are proposed. One corresponds to the formation of a nanodomain state, the second leads to a ferroelectric phase transition.

In Sec. 3 relaxational behaviour of a polar moment in an anisotropic double-well potential is analyzed. This analysis is aimed at understanding the influence of random fields on the relaxation of the polar clusters. The polar moment can be either a polarized unit cell or a polar cluster. A gen-

eral expression for the relaxation of a polar moment in a biassed local field and formulae for the calculation of dielectric response of relaxors are then deduced.

In Sec. 4 the dielectric response of PST and PMN is calculated as a function of temperature and frequency and compared with experimental results, under some assumptions about the size distribution of the polar clusters and the relaxation time.

2. Random fields and polar clusters

Our analysis[16,17] of the relationship between the chemical defect structures and the resulting electric field distributions showed very clearly that the spatial distribution of the local (random) fields is not totally random but contains some correlations in direction and strength. Thus Figs. 1(a,d) show e.g. two B-site cation distributions for a 1:1 ratio of B1 and B2. Calculated x- and y-components of the local electric fields are shown as Figs.1 (b,e) and (c,f) respectively, based on a Potts model simulation of the polar domain structures. The predominant chemical defects are domain walls, there are also a lower density of "point" and "line defects" within the chemical domains[12–14]. Thus the local electric fields tend to be much stronger at the chemical domain walls than is the case inside the domains. The local biassed electric field at such boundaries would be expected to strongly influence the formation and dynamics of polar clusters. We may consider these boundaries as extended defects with finite dimensions. We will refer to them here simply as defect-centers. The defect-centers in PMN should have a diameter approximately equal to the correlation length ξ_{chem} for 1:1 ordering of Mg^{2+} and Nb^{5+}. Similarly, for the case of PST, the sizes have diameter approximately equal to the correlation length ξ_{chem} for 1:1 ordering of Sc^{3+} and Ta^{5+}. The reader is referred to refs.[12–14] for details of the chemical domain structures and to ref.[15,16] for details of the simulations of the spatial relationships between the chemical and polar domain textures in PMN.

(a) Dynamical and frozen clusters

Now we examine the influence of these correlated local fields on the formation and dynamics of the polar clusters and nanodomains. It has been shown that the local polarization ($P_s^2 \neq 0$) exists for temperatures far above the temperature of the permittivity maximum T_m[18,19]. It has also been shown that the global symmetry of the low temperature phase of PMN remains cu-

bic even when the temperature was decreased down to 5K[20] which means no condensation of soft modes or long range lattice distortions and/or cation displacements occur for PMN. Hence, it is appropriate to describe the dielectric behaviour with an ensemble of interactive dipolar moments. Locally polar regions occur at low temperature (5K); these appear to have rhombohedral structure. One may assume that the dipolar moments take orientations along the eight ⟨111⟩ directions of the cubic Pm3m cell.

At high temperature ($T \gg T_m$), these dipolar moments are completely decoupled. As the temperature is decreased, some correlation among the dipolar moments will develop, i.e. polar clusters will form. Due to the presence of the compositionally induced local fields, the behaviours of the polar clusters will differ from point to point. A polar cluster controlled by a defect-center (chemical domain wall) will have a strong tendency to have polarization lined up along the direction of the local electric field. In the other regions the local polar clusters may experience almost zero bias field, hence they can continue flipping, virtually unhindered, exhibiting superparaelectric characteristics. Thus, we may distinguish essentially two kind of polar clusters at a given temperature, according to their dynamical characteristics. One type is essentially static, or at least relatively very low frequency, say 1–100 Hz, determined by the strength of the local field. We refer to these as frozen polar domains (FPD). Note that the existence of FPDs requires large random fields. The size of the FPDs is also determined by the correlation in direction of the random fields.

The second type of defect center is essentially dynamical, fluctuating over symmetrically and/or energetically equivalent polarization domain states. We refer to the latter as dynamical polar domains (DPD). In general, throughout some finite temperature range we may expect that there will be a mixture of FPDs and DPDs. Of course the proportions of FPDs and DPDs should vary systematically with temperature.

Assuming the polar correlation length at temperature T is $\xi_p(T)$ unit cells, then the number of unit cells involved in a dynamical polar cluster with average size is

$$s_{av}(T) = \xi_p^3(T)\,. \tag{1}$$

An alternative expression for the average size of the frozen polar clusters may be derived as follows. Assume defect-centers act as nuclei for the formation of frozen clusters. At higher temperature, $\xi_p(T)$ is much smaller than ξ_{chem}, hence the average size of the frozen polar clusters can be written as

$$s_f(T) = \xi_{chem}^2 \xi_p(T)\,. \tag{2}$$

As the temperature is decreased, while ξ_{chem} remains constant, $\xi_p(T)$ will

increase. The volume fraction of FPDs $c_f(T)$ will increase, and the space for dynamical polar clusters will decrease. If we assume the density of the defect-centers c_0 is a constant independent of temperature, then $c_f(T)$ can be expressed as

$$c_f(T) = c_0 \xi_{chem}^2 \xi_p(T) \,. \tag{3}$$

(b) Two kinds of competing percolation processes

At a certain temperature T_1, the polar correlation length will become comparable to the chemical correlation length, i.e.,

$$\xi_p(T_1) = \xi_{chem} \,.$$

If at this temperature T_1 the fraction of FPDs $c_f(T_1)$ is equal to or exceeds the percolation threshold at which the frozen polar clusters contact each other, forming a "percolation" cluster, a frustration will happen among the FPDs oriented along eight different $\langle 111 \rangle$ directions. Note that we assume eight $\langle 111 \rangle$ directions are activated for concreteness; in fact both the number and direction of local polar domains may be temperature dependent. Actually the analysis here and the results obtained so far are not dependent on this assumption. When this frustration occurs, the space for the dynamical polar domains is limited so that the polar correlation length $\xi_p(T)$ will stabilize at ξ_{chem} and a ferroelectric phase transition will never happen in a zero-field process. The system will finally freeze to a so-called random field stabilized domain state (Kleemann[11]). This may be just the case for PMN; T_1 corresponds to the frezinsg temperature (T_f)[7,8]. This type of percolation may not be detected in dielectric response measurements, because FPDs give no dispersive contribution to the dielectric response.

If the volume fraction of the FPDs $c_f(T)$ is still very small at temperature T_1, the polar correlations can develop further. The DPDs will compete with FPDs for space. Finally, the polar interaction may win the competition by forming a percolated polar cluster at a temperature T_c. Thus percolation occurs when all the DPDs plus 1/8 of the FPDs reach a percolation threshold. All the DPDs in the percolated cluster may then achieve the same polarization orientation as that of one set of FPDs. This percolation may actually be able to initiate the ferroelectric phase transition in the sense that macroscopic polar or ferroelectric domains form. The polar interaction may gain energy by forming larger compact polar domains and finally overcome the influence of the local random fields. Such large percolated clusters will then freeze out at the percolation threshold. Thus the dielectric response will have a sharp

drop at that point. This may be the case for disordered $Pb(Sc_{1/2}Ta_{1/2})O_3$[21,22] and $Pb(Sc_{1/2}Nb_{1/2})O_3$ which undergo spontaneous transformations from relaxor to ferroelectric states[22,23].

3. Relaxation of a polar moment in an anisotropic double-well potential

To predict a macroscopic property of a complex system, it is always desirable to simplify the many-body problem into a single-body problem in the style of Landau theory or mean field theory. As indicated in previous chapters, relaxors exhibit "super-paraelectric" characteristics which underlie the extremely high dielectric permittivity of relaxors. It is natural to choose these polar nanodomains as basic elements to calculate the macroscopic properties. However, the polar nanodomains are not really independent, interaction must occur among them when the temperature is decreased. Then we still have a many-body problem with these interacting nanodomains. Cluster concepts, which we adopted in refs.[16,17], avoid the interaction problem. Theee are defined within a bond-site correlated percolation problem. Due to the special way used to identify the clusters, each cluster has no interaction with the others. These clusters may have fractal geometry rather than the compact form of polar nanodomains. We can treat each cluster as a single polar moment completely decoupled from the remaining clusters of the system and calculate its contribution to the macroscopic property and then add them together to get the macroscopic property of the whole system.

To begin to understand the influence of random fields on the relaxation of the polar clusters, we first examine a simple case of a moment p in an anisotropic double-well potential (see Fig. 2). A weak electric field $\mathbf{E}$ is applied.

Suppose that the probabilities for the moment to be oriented in the two orientations are ϕ_1 and ϕ_2 respectively at a given time and that the probability of a moment flip from orientation 1 to orientation 2 in time δt is $w_{12}\delta t$, while the probability of the reverse process is $w_{21}\delta t$. Then

$$\begin{cases} d\phi_1/dt &= -w_{12}\phi_1 + w_{21}\phi_2 \\ d\phi_2/dt &= \quad w_{12}\phi_1 - w_{21}\phi_2 \end{cases} \tag{4}$$

In equilibrium $d\phi_1/dt = d\phi_2/dt = 0$; therefore we must have

$$\phi_1/\phi_2 = w_{21}/w_{12}.$$

However, in equilibrium ϕ_1 and ϕ_2 must satisfy the Boltzmann distribution,

so

$$\begin{cases} \phi_1 &= A\exp(-F_1/kT)\exp(pE/kT) \\ \phi_2 &= A\exp(-F_2/kT)\exp(-pE/kT) \end{cases}$$

where A is a constant and k is the Boltzmann constant. Hence, we can take

$$\begin{cases} w_{12} &= (1/2\tau_0)\exp(F_1/kT)\exp(-pE/kT) \\ w_{21} &= (1/2\tau_0)\exp(F_2/kT)\exp(pE/kT) \end{cases}$$

If $pE/kT \ll 1$, Eqs. (4) become

$$\begin{cases} d\phi_1/dt &= -(1/2\tau_1)(1-pE/kT)\phi_1 + (1/2\tau_2)(1+pE/kT)\phi_2 \\ d\phi_2/dt &= (1/2\tau_1)(1-pE/kT)\phi_1 - (1/2\tau_2)(1+pE/kT)\phi_2 \end{cases} \tag{5}$$

where we have taken

$$\tau_1 = \tau_0\exp(F_1/kT) \quad \text{and} \quad \tau_2 = \tau_0\exp(F_2/kT)\ , \tag{6}$$

where τ_0 is a characteristic time of the thermal agitation related to the Debye frequency. τ_1 and τ_2 are the two characteristic relaxational times of the anisotropic double wells The 'net' probability for a moment to be oriented up (orientation 1) is $\varphi = \phi_1 - \phi_2$. Noting that $\phi_1 + \phi_2 = 1$, from Eqs. (5) we have

$$\frac{d\varphi}{dt} = \frac{\tau_1-\tau_2}{2\tau_1\tau_2} - \frac{\tau_1+\tau_2}{2\tau_1\tau_2}\frac{pE}{kT} + \frac{\tau_1+\tau_2}{2\tau_1\tau_2}\varphi - \frac{\tau_1-\tau_2}{2\tau_1\tau_2}\frac{pE}{kT}\varphi \tag{7}$$

If E varies with time as $E_0\exp(i\omega t)$ and assuming the above equation has solution

$$\varphi = \sum_n c_n\exp(in\omega t)$$

we obtain

$$\begin{aligned} c_0 &= \frac{\tau_1-\tau_2}{\tau_1+\tau_2}\ , \\ c_n &= c_{n-1}\left(\frac{pE_0}{kT}\right)\frac{1/\tau_1 - 1/\tau_2}{i2n\omega + 1/\tau_1 + 1/\tau_2}\ . \end{aligned}$$

Neglecting the $n > 1$ terms of $\exp(in\omega t)$, we have the solution

$$\varphi = \frac{\tau_1-\tau_2}{\tau_1+\tau_2} + \frac{pE}{kT}\frac{1}{(\tau_1+\tau_2)^2/4\tau_1\tau_2 + i\omega(\tau_1+\tau_2)/2} \tag{8}$$

When $\tau_1 = \tau_2$, this becomes the familiar Debye relaxation form

$$\varphi = \frac{pE}{kT}\frac{1}{1+i\omega\tau}$$

If the origin of the anisotropy is coming from the local random field $\mathbf{E}_l$, we can write $F_1 = F_0 + F_a$ and $F_2 = F_0 - F_a$, where

$$F_a = \mathbf{p} \cdot \mathbf{E}_l \,, \tag{9}$$

and F_0 is the well depth. If $\mathbf{p}$ represents the dipolar moment of a polar cluster, F_0 should be proportional to the cluster size s. Thus, we write

$$F_0 = s g_0 \,, \tag{10}$$

where g_0 is the energy barrier between two adjacent orientations of the local polarization of a unit cell. Substituting Eqs. (6) into Eq. (7), we find that φ takes the form

$$\varphi = \tanh(F_a/kT) + \frac{pE_0}{kT} \frac{\cosh^{-2}(F_a/kT)}{1 + i\omega\tau_0 \exp(F_0/kT)/\cosh(F_a/kT)} \,. \tag{11}$$

This is the general expression for the relaxation of a dipolar moment in an anisotropic double-well potential.

If the dielectric behaviour of a system can be described by a large number of independent polar clusters with dipolar moments p_i ($i = 1, 2, 3, ..., N_p$), the polarization of the system is then

$$P = \sum_i^{N_p} \langle p_i \rangle / (N v_0),$$

where N is the total number of unit cells in the system and v_0 is the volume of the unit cell. The complex permittivity can be written

$$\chi(T, \omega) = \sum_i^{N_p} \chi_i \,, \tag{12}$$

where χ_i is the contribution of the moment p_i to the total permittivity of the system; thus

$$\chi_i = \left(\frac{p_i^2}{N \varepsilon_0 v_0 kT} \right) \frac{\cosh^{-2}(F_a/kT)}{1 + i\omega\tau_0 \exp(F_0/kT)/\cosh(F_a/kT)} \,, \tag{13}$$

where ε_0 is the vacuum dielectric constant. If $F_a/kT \ll 1$, we have

$$\chi_i = \left(\frac{p_i^2}{N \varepsilon_0 v_0 kT} \right) \frac{1}{1 + i\omega\tau_0 \exp(F_0/kT)} \,. \tag{14}$$

Here we refer to the dynamical polar clusters or DPDs. This kind of polar cluster or domain will give the most significant contribution to the dielectric response. If $F_a/kT \gg 1$, then $\chi_1 \sim 0$, which means the moment is almost fixed by the local bias field and this case gives little contribution to the permittivity. The relaxational time τ_1 is much larger than τ_2; τ_1 is the dominant characteristic relaxation time. This corresponds to the frozen polar clusters or FPDs.

In relaxor PMN or PST, there exist eight possible orientations under the assumption of rhombohedral symmetry. The result for χ_i is similar to that of a double-well potential. In the case $\mathbf{E}_l \sim 0$, and assuming the flipping only occurs between two adjacent orientations, we have

$$\chi_i = \left(\frac{p^2}{3\varepsilon_0 V kT}\right) \frac{1}{1 + i\omega\tau_0 \exp(F_0/kT)} \,. \tag{15}$$

This differs from Eq. (5.14) by just a factor 1/3. Further details of the derivation are given in the Appendix.

4. Calculation of Dielectric Permittivity

In this section we use the model and formulae developed in the above two sections to calculate the permittivity of PMN and PST. The dispersive and relaxational behaviours of the dielectric permittivity of PMN and PST can be attributed to the size dispersion and relaxation of the dynamic polar clusters. The average size $s_{av}(T)$ of the clusters is temperature dependent. The interactions among the polarised unit cells have already been taken into account in $s_{av}(T)$. Hence we may treat the polar clusters as independent of each other.

(a) Cluster Size and Correlation Length

The average size $s_{av}(T)$ of dynamical clusters can be expressed in term of polar fluctuation correlations (Eq. (1)). For a genuine ferroelectric phase transition, the polar correlation length will diverge as T_c is approached. It usually takes the form

$$\xi_p(T) \sim (T - T_c)^{-\mu} \tag{16}$$

The situation in relaxors is different. For example, the correlation length in PMN becomes nearly temperature independent as the temperature is decreased[24,25]. The simulation results in ref.[16,17] also show this tendency in systems with correlated random fields. It will be helpful if we have an

analytical expression for the correlation length as a function of temperature. Fig. 3 shows the neutron diffraction results for PMN and the fitting curve using

$$\xi_p(T) = \xi_p(\infty) + \frac{\xi_p(0) - \xi_p(\infty)}{2}\Big[1 + \tanh[\theta(1 - T/T_0)]\Big]. \qquad (17)$$

The fitting parameters are: low temperature correlation length $\xi_p(0) = 21.1$ nm, high temperature correlation length $\xi_p(\infty) = 3.8$ nm, $T_0 = 300$ K, and $\theta = 3$. T_0 is the temperature at which significant correlation of the local polar moments starts to develop. Between temperature T_0 and the freezing temperature T_f[6], PMN exhibits typical relaxational behaviour.

Disordered PST and PSN exhibit a so-called spontaneous relaxor to ferroelectric phase transition. They first show typical relaxor behaviour when temperature is decreased, but a spontaneous polarization appears at temperature T_c. Hence the correlation length for disordered PST and PSN may take the form of a combination of Eq. (16) and Eq. (17), i.e. the correlation length takes the form of Eq. (16) when $T > T_1$, and it takes the form of Eq. (17) when $T < T_1$.

(b) Static permittivity of PMN

First we consider the static permittivity, i.e. take $\omega = 0$ in Eq. (13). Then we have

$$\chi_i = \frac{p_i^2}{N\varepsilon_0 v_0 kT}\frac{1}{\cosh^2(F_a/kT)}\,. \qquad (18)$$

Note that the factor $1/\cosh^2(F_a/kT)$ will decrease sharply when F_a/kT increases; it equals 0.42 when $F_a/kT = 1$ and it becomes 0.07 when $F_a/kT = 2$. Hence, we use the simple model discussed in Sec. 2(a) and just distinguish two kinds of clusters, dynamic and frozen, according to the value of F_a. For example, if $F_a/kT > 1$ the cluster is classified as FPD and $\chi_i = 0$; if $F_a/kT < 1$ the cluster is DPD and $\chi_i = p_i^2/(N\varepsilon_0 v_0 kT)$.

Eq. (3) gives the volume fraction of FPDs, $c_f(T)$, at temperature T. Let $c_{f0} = c_0\xi_{chem}^2$, then $c_f(T) = c_{f0}\xi_p(T)$. The number of dynamical polar clusters with size $s_{av}(T)$ in the system is then $(1 - c_{f0}\xi_p(T))N/s_{av}(T)$. For a polar cluster with size $s_{av}(T)$, the dipolar moment is $p = s_{av}(T)p_0$, where p_0 is the dipolar moment of the local polarization of a unit cell. Thus, the static permittivity of the system can be written

$$\chi_s(T) = A_0\frac{(1 - c_{f0}\xi_p(T))s_{av}(T)}{T}\,, \qquad (19)$$

where

$$A_0 = \frac{p_0^2}{3\varepsilon_0 v_0 k} .$$

We have added a 1/3 factor in A_0 because Eq. (15) is preferable to Eq. (14) for a system with eight orientations like PMN. Substituting Eqs. (1) and (17) into Eq. (19), we calculate $\chi_s(T)$ of PMN as a function of temperature. Fig. 4 shows the result; we have taken $c_{f0} = 1/\xi_p(0) = 0.019$, the unit cell parameter $a_0 = 0.4$ nm, and $p_0 = 3.0 \times 10^{-30}$ Cm so that $A_0 = 380$ K.

The temperature dependence of the static permittivity of PMN (Fig. 4) can be well explained by the percolation model proposed in Sec. 2(b). The FPDs will give little contribution to the permittivity $\chi_s(T)$ if the applied electric field is very weak. When the percolation threshold of the FPDS is approached, FPDs will dominate the space and the volume proportion of the DPDs undergoes a sharp decrease. Finally, the system will freeze into a polar domain state. The average size of the frozen polar domains is predetermined by the parameter c_{f0} which reflects the frozen structure of the chemical nanodomains of the B-site cations and other defects.

(c) Dynamic Permittivity

Because the relaxational time of a dynamic polar cluster is also related to its size, we need to consider the size distribution of the DPDs at a temperature T. The cluster-size distribution is typically expressed as a discrete function $n(s) = N_s(s)/N_t$, defined at $s = 1, 2, 3, 4, \ldots$, where $N_s(s)$ is the number of clusters with size s and N_t is the total number of sites. In our problem N_t is the total number of unit cells occupied by the dynamic clusters. Hence, $N_t = N(1 - c_{f0}\xi_p(T))$, which means we will not consider the contribution of the FPDs to the permittivity (in weak applied field).

The probability to find a site to be in a cluster with size s is $sn(s)$. We assume without proof that $sn(s)$ has the Gaussian distribution,

$$sn(s) = \frac{1}{\sqrt{2\pi}\sigma} \exp(-(s - s_{av})^2/2\sigma^2) . \qquad (20)$$

This assumption is justified for a relaxor system because the average domain size is nanoscale in the temperature range of interest, far away from a site-bond percolation threshold (i.e. a ferroelectric transition). The question of suitable cluster distributions was investigated by Chamberlin[26–28] in his "dynamically coupled domain" theory. In the temperature range of interest, $s_{av}(T) \gg 1$. If we take a suitable value for σ, $N_s(s)$ will actually be 0 when

$s \leq 0$. Hence, the following conditions are satisfied:

$$\sum_{s=1}^{N} sn(s) \sim \int_{-\infty}^{\infty} [sn(s)]ds = 1 \ , \tag{21}$$

and

$$\sum_{s=1}^{N} s^2 n(s) \sim \int_{-\infty}^{\infty} [sn(s)]sds = s_{av} \ . \tag{22}$$

As a further assumption we let $\sigma = \gamma s_{av}$, where γ is a constant which will be one of the adjustable parameters in later calculations. Fig. 5 shows the size distributions of PMN at temperature 450 K, 400 K and 350 K when $\gamma = 0.33$.

The contribution of a dynamical cluster with size s and dipolar moment sp_0 to the complex permittivity can be written as

$$\chi_1(T, \omega, s) = \chi_1^{'}(T, \omega, s) - i\chi_1^{''}(T, \omega, s)$$

From Eq. (15) we have

$$\chi_1^{'}(T, \omega, s) = \left(\frac{A_0}{N}\right) \frac{s^2/T}{1 + (\omega\tau_0)^2 \exp(2bs/T)} \ , \tag{23}$$

and

$$\chi_1^{''}(T, \omega, s) = \left(\frac{A_0}{N}\right) \frac{\omega\tau_o \exp(bs/T)s^2/T}{1 + (\omega\tau_0)^2 \exp(2bs/T)} \ , \tag{24}$$

where $b = g_0/k$. We can obtain the permittivity of the system by adding the contributions of all the DPDs. The number of DPDs with size s is $N(1 - c_{f0}\xi_p(T))n(s)$, hence we have

$$\chi^{'}(T, \omega) = A_0 \frac{(1 - c_{f0}\xi_p(T))}{T} \int_1^{\infty} \frac{sn(s)sds}{1 + (\omega\tau_0)^2 \exp(2bs/T)} \ , \tag{25}$$

for the real component of permittivity and

$$\chi^{''}(T, \omega) = A_0 \frac{(1 - c_{f0}\xi_p(T))}{T} \int_1^{\infty} \frac{\omega\tau_0 \exp(2bs/T)sn(s)sds}{1 + (\omega\tau_0)^2 \exp(2bs/T)} \ , \tag{26}$$

for the imaginary permittivity of the system respectively. It is interested to note that the above results (Eq. 25 and Eq. 26) are essentially the same formulae as given by Chamberlin in his congenial work on ferromagnetic materials[26–28].

(d) Results for PMN

Substituting Eqs. (1), (17), and (20) into Eqs. (25) and (26), we can calculate the real and imaginary permittivity of PMN. Fig. 5 (a) and (b) show respectively the calculated results for permittivity and dissipation factor of PMN as a function of temperature at frequencies 1k, 10k, 100k, 1M Hz. We have taken $A_0 = 380$, $c_{f0} = 0.019$ as before, $b = 0.1$K and $\tau_0 = 10^{-12}$s. For polar clusters with diameter 5 nm ($s = 1953$), the activation energy $F_0 = sg_0 = skb = 0.015$ eV.

The calculated permittivity and dissipation factor in Fig. 5 are in good agreement with the experimental measurements (see for example, Fig. 1(a) and (b) of Ye and Schmid[29] and Fig. 1(a) of Viehland et al[7]. Note that we did not adjust the parameters of Eq. (17) in our calculations. Actually we only made some adjustment on A_0 and b and γ. By modifying the parameters of Eq. (17) or just using $\xi_p(T)$ as a parameter and employing more sophisticated procedures, one may expect to be able to quantitatively fit the experimental measurements of the dielectric permittivity and dissipation factor.

(e) Results for disordered PST

For disordered PST (PST-d) the variation of correlation length with temperature is assumed to take a form of combination of Eq. (16) and Eq. (17). The relaxor behaviour begins to be significant around temperature 320 K and the relaxor–ferroelectric phase transition temperature is $T_c = 269$K[22]. Hence the polar correlation length of PST-d is assumed to be

$$\xi_p(T) = \begin{cases} 29.55 + 23.04 \tanh[3.2(1 - T/320)] & \text{if } T \geq 300\text{K} \\ 3.9(T - 269)^{-1} & \text{if } T < 300\text{K} \end{cases} \tag{27}$$

which is graphed in Fig. 6. Fig. 7 shows the calculated results for the permittivity as a function of temperature at frequencies 100, 1k 10K, 100k and 1M Hz respectively. The results are at least qualitatively in agreement with experimental results (see for example Fig. 4 of ref.[22]). The calculated result for PST is not as good as for PMN, which is mainly due to the rough assumption applied for $\xi_p(T)$. Using $\xi_p(T)$ as a fitting parameter one may expect to obtain curves which quantitatively agree with experimental results.

5. Discussion

The phenomenological theory presented in this paper covers the whole temperature range of interest in a unified form. The leading relaxation time of the polar cluster fluctuation is $t = \tau_0 \exp[s_{av}(T)g_0/kT)]$ at a temperature T. When T is significantly above T_{max}, $s_{av}(T)$ varies very slowly with temperature and thus the dielectric relaxation is Debye-like[30]. In the temperature region around T_m, $s_{av}(T)$ changes quickly with temperature, which results a non-Debye relaxation. Due to the effect of the random fields originated from nanoscale chemical defects, $s_{av}(T)$ will stabilize at a certain stage when the temperature is decreased and hence a random-field stabilized domain state forms, as predicted by Kleemann[11].

Acknowledgements

This work was supported financially be the Australian Research Council and the Australian Equity and Merit Scholarship Scheme.

References

[1] L.E. Cross, *Ferroelectrics* **76**, 241-267 (1987).
[2] L.E. Cross, *Ferroelectrics* **151**, 305-320 (1994).
[3] J. Chen, H.M. Chan and M. Harmer, *J. Am. Ceram. Soc.*, **72**, 593-598 (1989).
[4] C.A. Randall, D.J. Barber and R.W. Whatmore, *J. Micros.*, **145**, 275-291 (1987).
[5] D. Viehland, J.J. Li, S.J. Jang, L.E. Cross and M. Wuttig, *Phys Rev. B*, **43**, 8316-8320 (1991).
[6] D. Viehland, S.J. Jang, L.E. Cross and M. Wuttig, *J. Appl. Phys.*, **68**, 2916-2921 (1990).
[7] D. Viehland, S.J. Jang, L.E. Cross and M. Wuttig, *Philos. Mag.*, **B64**, 335-344 (1991a).
[8] D. Viehland, S.J. Jang, L.E. Cross and M. Wuttig, *J. Appl¿ Phys.*, **69**, 414-419 (1991b).
[9] D. Viehland, M. Wuttig and L.E. Cross, *Ferroelectrics*, **120**, 71-77 (1991).
[10] V. Westphal, W. Kleemann and M.D. Glinchuk, *Phys. Rev. Lett.*, **68**, 847-850 (1992).
[11] W. Kleemann, *Inter. J. Mod. Phys. B*, **13**, 2469-2507 (1993).
[12] L.A. Bursill, J.L. Peng, H. Qian and N. Setter, *Physica B*, **205**, 305-326 (1995).
[13] L.A. Bursill, H. Qian, J.L. Peng and X.D. Fan, *Physica B*, **216**, 1-23 (1995).
[14] H. Qian, J.L. Peng and L.A. Bursill, *Inter. J. Mod. Phys. B*, **7**, 4353-4369 (1993).
[15] G. Smolenskii and V.A. Isupov, *Dolk. Akad. Nauk SSSR*, **9**, 653-660 (1954).
[16] H. Qian and L.A. Bursill, "A random-field Potts model for perovskite-type relaxor ferroelectrics", *Inter. J. Mod. Phys. B*, submitted (1996).
[17] H. Qian, Ph.D Thesis, School of Physics, University of Melbourne (1996).
[18] G. Burns and F.H. Dacol, *Phys. Rev. B*, **28**, 2527-2530 (1983).
[19] G. Burns and F.H. Dacol, *Ferroelectrics*, **104**, 25-31 (1990)
[20] N. de Mathan, E. Husson, G. Galvarin, J.R. Gavarri, A.W. Hewat and A. Morell, *J. Phys.: Cond. Matter*, **3**, 8159-8171 (1991).
[21] L.A. Bursill, J.L. Peng and H. Qian, in "Science of Ceramic Interfaces II, (J Nowotny, Ed.), *Materials Science Monographs* **81**, 441-471 (Elsevier, Amsterdam) (1994).

[22] F. Chu, I.M. Reaney and N. Setter, *Ferroelectrics*, **151**, 343-348(1994).
[23] F. Chu, I.M. Reaney and N. Setter, *J. Appl. Phys.*, **77**, 1671-1676 (1995).
[24] S.D. Vakhrushev, B.E. Kvyatkovskyi, A.A. Naberezhnov, N.M. Okuneva and B.P. Toperverg, *Ferroelectrics*, **90**, 173-176 (1989).
[25] E.V. Colla, E. yu Koroleva, N.M. Okuneva and S.B. Vakhrushev, *J. Phys.: Cond. Matter*, **4**, 3671-3677 (1993).
[26] R.V. Chamberlin and D.N. Haines, *Phys. Rev. Letts.*, **65**, 2197-2199, (1990).
[27] R.V. Chamberlin, *Phys. Rev.*, **48**, 15638-15645 (1993).
[28] R.V. Chamberlin and M.R. Scheinfein, *Science*, **260**, 1098-1101 (1993).
[29] Z.G. Ye and H. Schmid, *Ferroelectrics*, **145**, 83-99 (1993).
[30] O. Kersten, A. Rost and G. Schmidt, *Physica Status Solidi (a)*, **75**, 495-503, (1983).

Appendix

Consider a polar system with eight possible orientations along the ⟨111⟩ directions of the cubic Pm3m cell. Suppose that the probabilities for a moment to be oriented in one of the orientations i is ϕ_i at a given time and that a moment flip from orientation i to orientation j has a probability $w_{ij}\delta t$. A weak external field $E = E_0 \exp(i\omega t)$ is applied along one of the orientations (say, orientation 1). Assume the flippings of the polar moments occur only via the nearest orientations, i.e. 1 to 3, 5, 7; 2 to 1, 6, 8; 4 to 2, 5, 7; 5 to 1, 4, 8; 6 to 2, 3, 7; 7 to 1, 4, 6; and 8 to 2, 3, 5 respectively. If one assigns indices to the orientations as shown in Fig. 9, then one can write

$$\begin{cases} d\phi_1/dt &= -(w_{13}+w_{15}+w_{17})\phi_1 + w_{31}\phi_3 + w_{51}\phi_5 + w_{71}\phi_7 \\ d\phi_2/dt &= -(w_{24}+w_{26}+w_{28})\phi_2 + w_{42}\phi_4 + w_{62}\phi_6 + w_{82}\phi_8 \\ d\phi_3/dt &= -(w_{31}+w_{36}+w_{38})\phi_3 + w_{13}\phi_1 + w_{63}\phi_6 + w_{83}\phi_8 \\ d\phi_4/dt &= -(w_{42}+w_{45}+w_{47})\phi_4 + w_{24}\phi_2 + w_{54}\phi_5 + w_{74}\phi_7 \\ d\phi_5/dt &= -(w_{51}+w_{54}+w_{58})\phi_5 + w_{15}\phi_1 + w_{45}\phi_4 + w_{85}\phi_8 \\ d\phi_6/dt &= -(w_{62}+w_{63}+w_{67})\phi_6 + w_{26}\phi_2 + w_{36}\phi_3 + w_{76}\phi_7 \\ d\phi_7/dt &= -(w_{71}+w_{74}+w_{76})\phi_7 + w_{17}\phi_1 + w_{47}\phi_4 + w_{67}\phi_6 \\ d\phi_8/dt &= -(w_{82}+w_{83}+w_{85})\phi_8 + w_{28}\phi_2 + w_{38}\phi_3 + w_{58}\phi_5 \end{cases} \tag{28}$$

Considering the equilibrium condition of the Boltzmann distribution, one can assume

$$\begin{aligned} w_{ij} &= \frac{1}{\tau_{ij}} \exp(-\mathbf{p}_i \cdot \mathbf{E}/kT) \\ &\simeq \frac{1}{\tau_{ij}} (1 - \mathbf{p}_i \cdot \mathbf{E}/kT) \end{aligned} \tag{29}$$

where τ_{ij} are the characteristic times. This can be written as

$$\tau_{ij} = \tau_0 \exp(-F_{ij}/kT)$$

where F_{ij} is the energy barrier from orientation i to orientation j. In the case of $\mathbf{E}_l \sim 0$, the lattice has cubic symmetry and all the F_{ij} between two nearest orientations will be the same, so one has $\tau_{ij} = \tau = \tau_0 \exp(F_0/kT)$. The flipping probabilities w_{ij} can then be written as w_i, where $w_1 = (1 - pE/kT)/\tau$, $w_2 = (1 + pE/kT)/\tau$, $w_3 = w_5 = w_7 = (1 - pE/3kT)/\tau$ and $w_4 = w_6 = w_8 = (1 + pE/3kT)/\tau$. The 'net' probability for a moment to be oriented in the direction of the applied electric field is

$$\varphi_z = \phi_1 - \phi_2 + (\phi_3 + \phi_5 + \phi_7 - \phi_3 - \phi_5 - \phi_7)/3 \, .$$

From Eqs 28 one obtains

$$\tau \frac{d\varphi_z}{dt} = -\varphi_z + \frac{pE}{3kT} , \tag{30}$$

where the condition $\sum_{i=1}^{8} \phi_i = 1$ has been used. The solution of Eq. 5.30 is

$$\varphi_z = \left(\frac{pE_0}{3kT}\right) \frac{1}{1 + i\omega\tau_0 \exp(F_0/kT)} . \tag{31}$$

Figure Captions

Figure 1.
Two kinds of B-site cation distributions with 1:1 ratio of B1 to B2 (a,d) and the calculated x (b,e) and y (c,f) components of the local electric fields. Note that the field is strongest at the chemical domain walls.

Figure 2.
Diagram illustrating an anisotropic double-well potential with two different depths of well F_1 and F_2.

Figure 3.
Correlation length of ferroelectric fluctuations as a function of temperature, experimental data and curve fitting with Eq. (13).

Figure 4.
Static Permittivity of PMN as a function of temperature as calculated from Eq. (15).

Figure 5.
Diagram illustrating the proposed Gaussian distribution of the size of dynamic polar clusters at temperatures 450 K, 400 K and 350 K respectively.

Figure 6.
Calculated dielectric permittivity (a) and dissipation factor (b) versus temperature at frequencies of 1K, 10K, 100K and 1M Hz for PMN.

Figure 7.
Assumed polar correlation length of disordered PST as a function of temperature.

Figure 8.
Calculated dielectric permittivity versus temperature at frequencies of 100, 1K, 10K, 100K and 1M Hz for PST.

Figure 9.
Diagrams shows the eight possible polar orientations of the Pm3m cubic cell and the numbering used in the appendix.

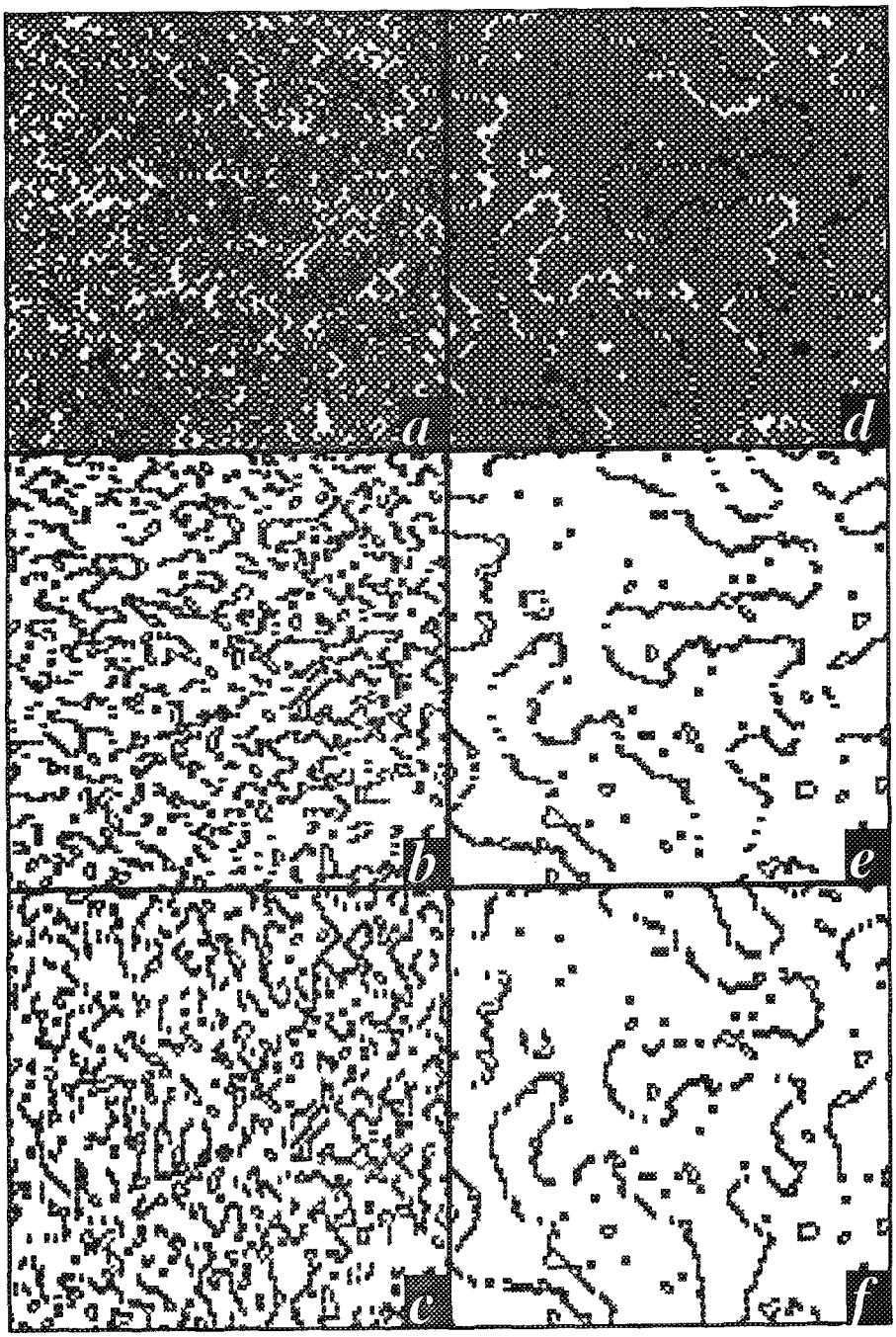

Figure 0.1: Two kinds of B-site cation distribution with 1:1 ratio of B1 and B2 ((a) and (d)) and the calculated x ((b) and (e)) and y ((c) and (f)) components of local elecric fields. See text for details.

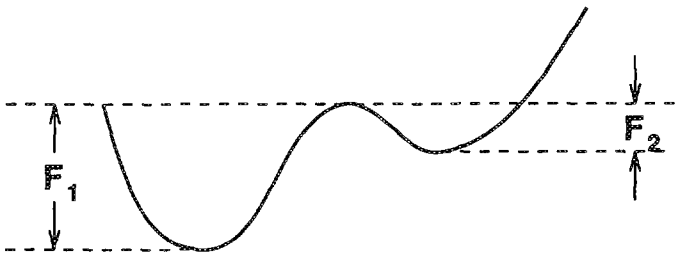

Figure 0.2: Diagram illustrating an anisotropic double-well potential with two different depths of well F_1 and F_2.

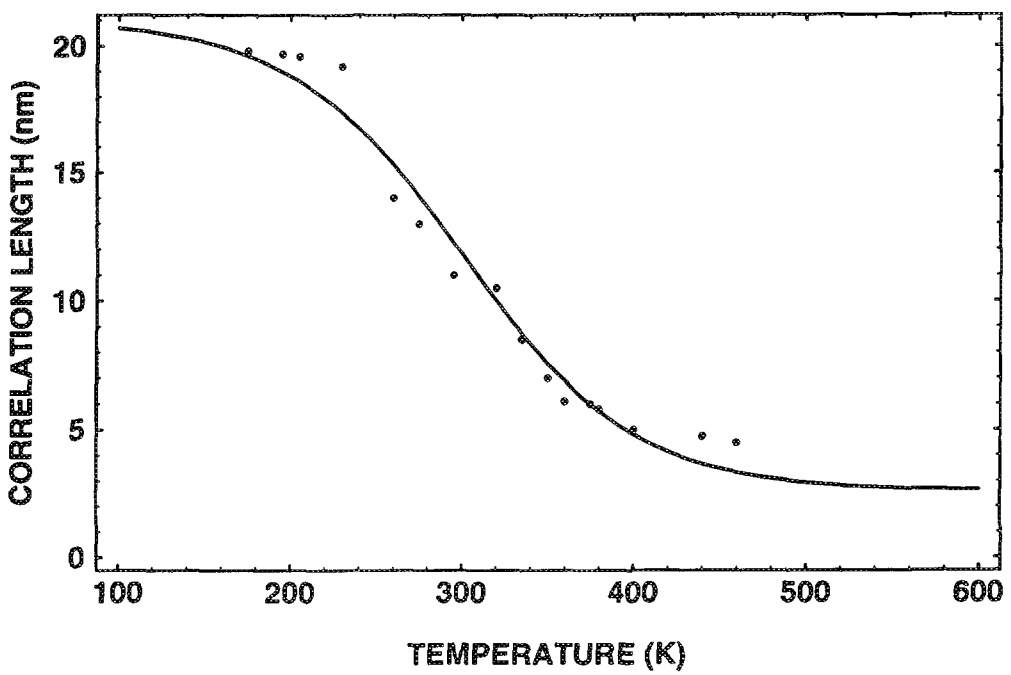

Figure 0.3: Correlation length of ferroelectric fluctuation as a function of temperature, experimental data and fitting curve with Eq. (17).

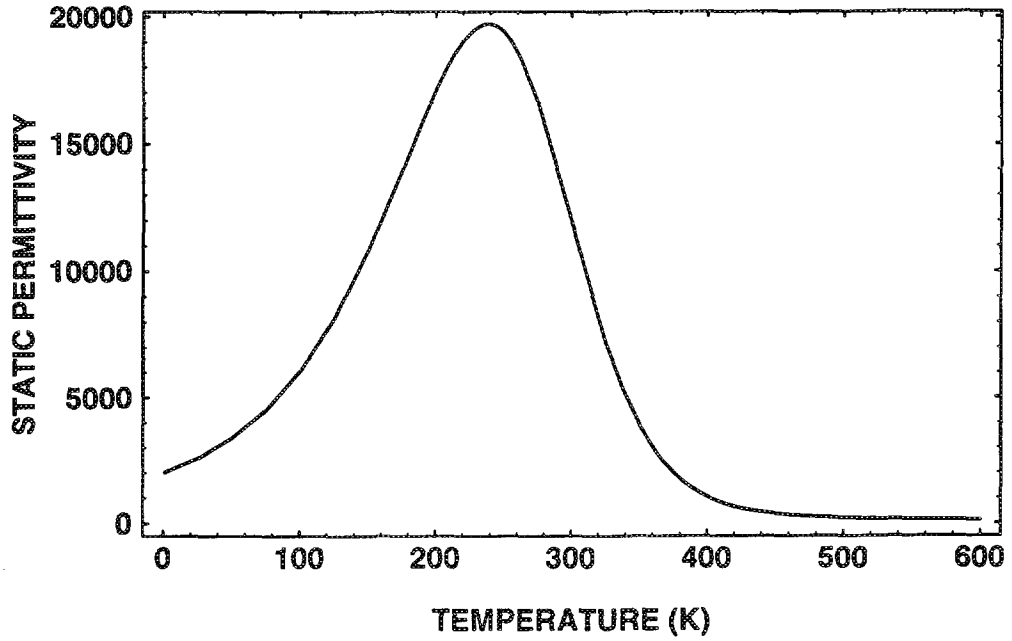

Figure 0.4: Static Permittivity of PMN as a function of temperature as calculated from Eq. (19).

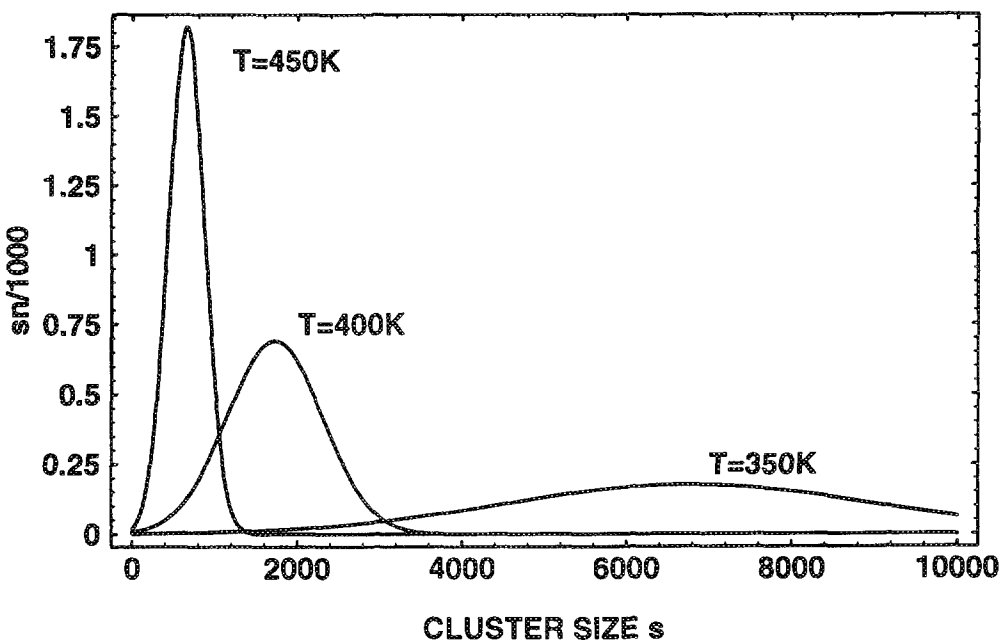

Figure 0.5: Diagram illustrating the proposed Gaussian distribution of the size of dynamic polar clusters at temperatures 450 K, 400 K and 350 K respectively.

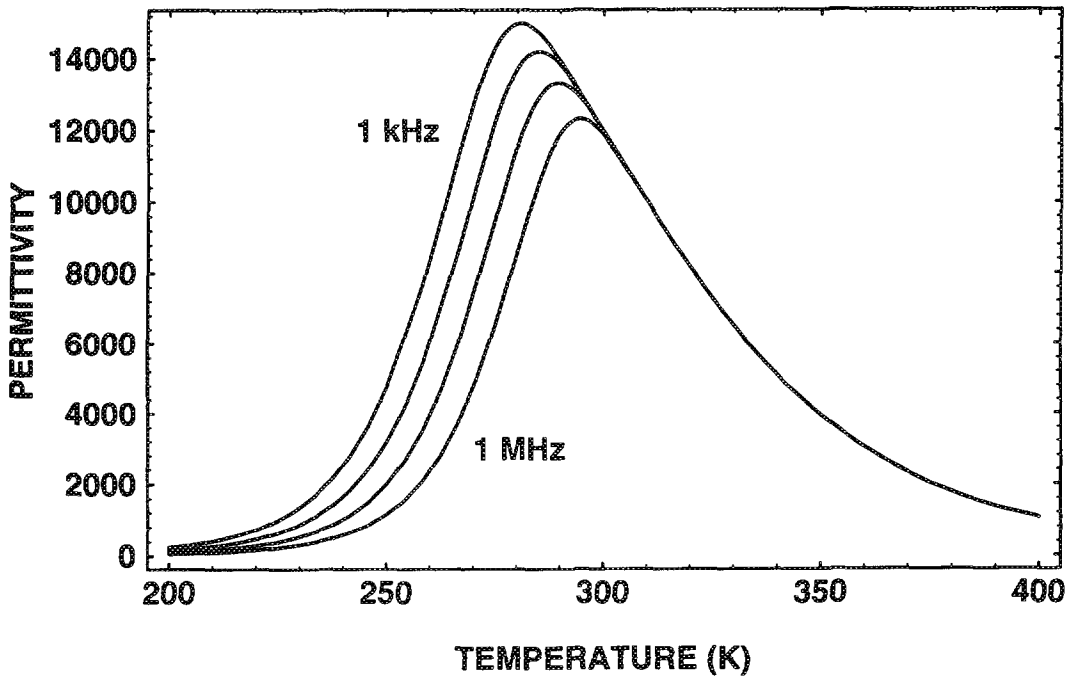

(a)

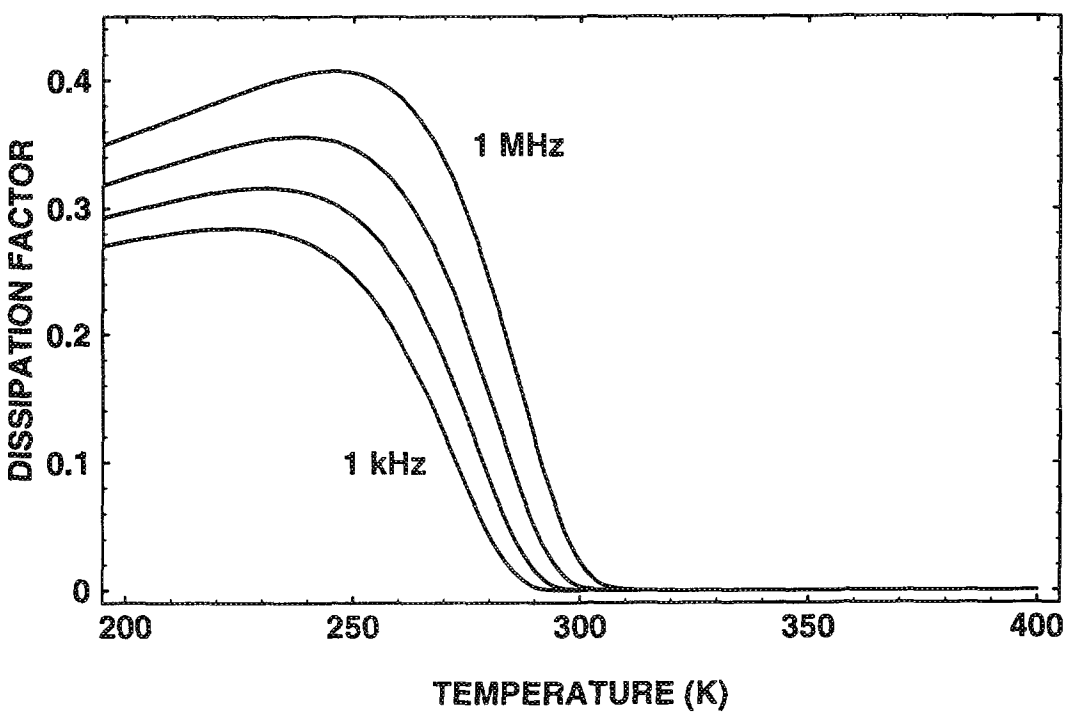

(b)

Figure 0.6: Calculated dielectric permittivity (a) and dissipation factor (b) versus temperature at frequencies of 1K, 10K, 100K and 1M Hz for PMN.

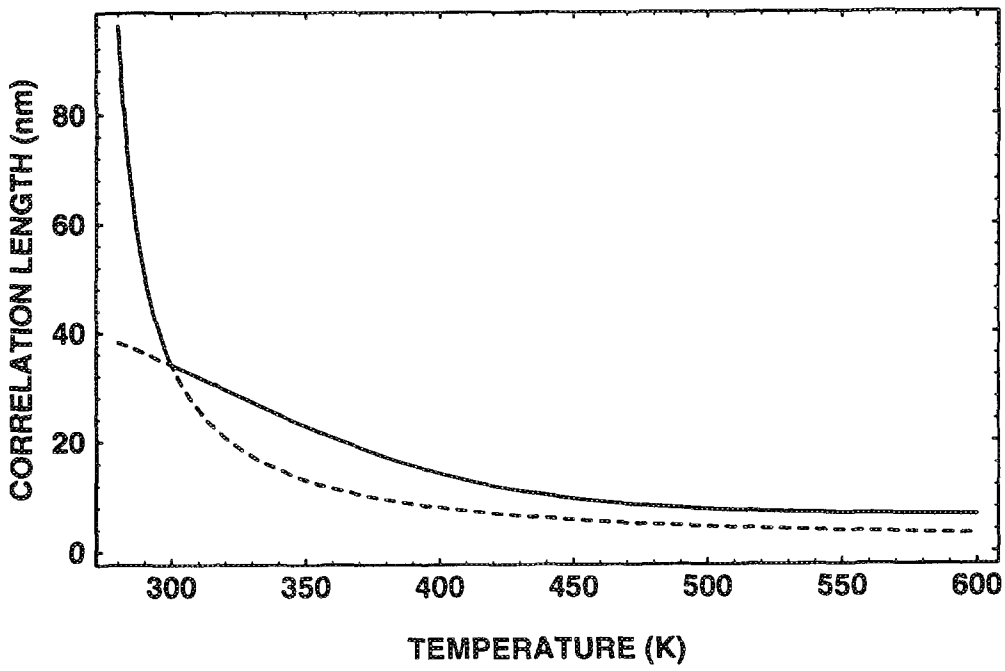

Figure 0.7: Assumed polar correlation length of disordered PST as a function of temperature.

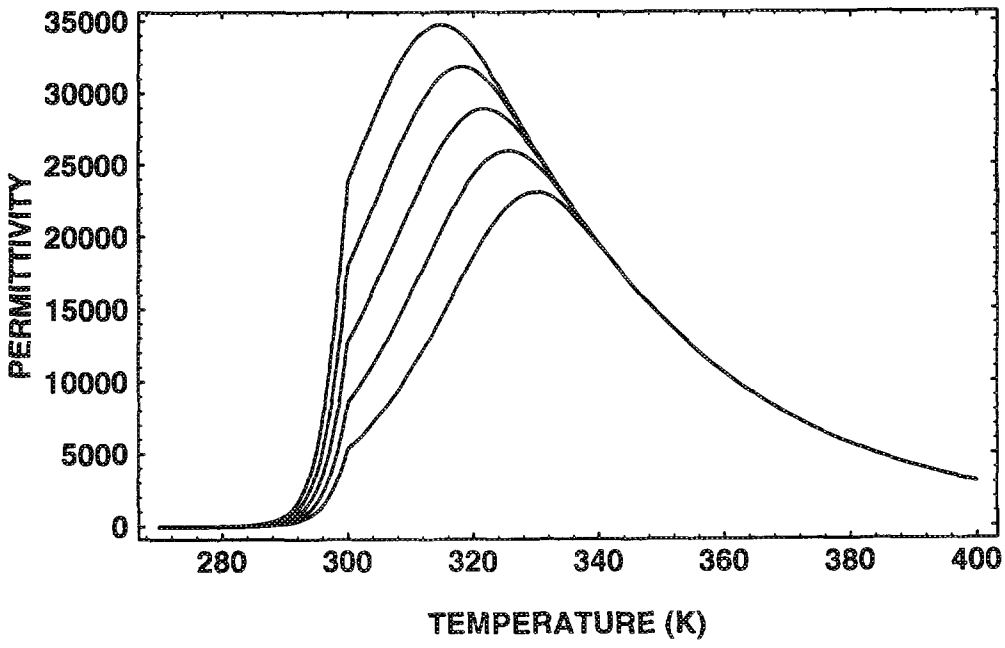

Figure 0.8: Calculated dielectric permittivity versus temperature at frequencies of 100, 1K, 10K, 100K and 1M Hz for PST.

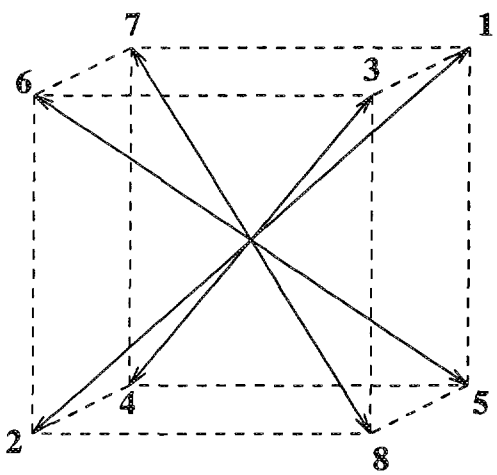

Figure 0.9: Diagrams shows the eight possible polar orientations of the Pm3m cubic cell and the numbering used in the appendix.